Clinical Imaging xxx (2013) xxx–xxx

Contents lists available at SciVerse ScienceDirect

Clinical Imaging

journal homepage: http://www.clinicalimaging.org

How reliable is MRCP with an SS-FSE sequence at 3.0 T: comparison between SS-FSE BH and 3D-FSE BH ASSET sequences

Eleftherios Lavdas [a,b,*], Marianna Vlychou [a], Nikolaos Arikidis [a], Eftychia Kapsalaki [a], Violeta Roka [a], Dimitrios L. Arvanitis [c], Ioannis Fezoulidis [a], Katerina Vassiou [a,c]

[a] Department of Radiology, University Hospital of Larissa, Greece
[b] Department of Medical Radiological Technological, Technological Education, Institute of Athens
[c] Department of Anatomy, School of Health Science, University of Thessaly

ARTICLE INFO

Article history:
Received 4 September 2012
Received in revised form 11 December 2012
Accepted 17 January 2013
Available online xxxx

Keywords:
Biliary system
Liver
3.0 T
MRCP
Pancreatic system
Pancreatic–Biliary system

ABSTRACT

Purpose: The purpose of the present study was to evaluate the visibility and the image quality of the biliary and pancreatic duct system on magnetic resonance cholangiopancreatography (MRCP) images based on two breath-hold (BH) methods using array spatial sensitivity technique: a single-shot fast spin-echo (SS-FSE) sequence and a three-dimensional single slab fast spin-echo (3D-FSE) sequence. **Materials and methods:** In the present prospective comparative study, 47 patients (22 male and 25 female, mean age=50 years, age range=22–82 years) that were referred for MRCP during a 12-month period are included. All of them were referred with suspected pancreaticobiliary disease. All patients underwent MRCP with both a SS-FSE BH sequence and a 3D-FSE BH sequence. Qualitative evaluation regarding the depiction of three segments of the pancreaticobiliary tree and the frequency of artifacts was performed. Two radiologists graded each sequence of the obtained studies in a blinded fashion. Quantitative evaluation including calculation of relative signal intensity (rSI) and relative contrast (RC) ratios at seven segments of the pancreaticobiliary tree between fluid-filled ductal structures and organ parenchyma at the same ductal segments was performed. In order to evaluate the parameters' differences of the two sequences, either in qualitative or in quantitative analysis, the Wilcoxon paired signed-rank test was performed. **Results:** On quantitative evaluation, both rSI and RC ratios of all segments of the pancreaticobiliary tree at SS-FSE BH sequence were higher than those at 3D-FSE BH sequences. This finding was statistically significant ($P<.01$). On qualitative evaluation, the two radiologists found intrahepatic ducts and pancreatic ducts to be better visualized with SS-FSE BH than with 3D-FSE BH sequence. This finding was statistically significant ($P<.02$). One of them found extrahepatic ducts to be significantly better visualized with SS-FSE BH sequence. Moreover, the frequency of artifacts was lower in the SS-FSE sequence, a finding that was of statistical significance. Interobserver agreement analysis found at least substantial agreement ($\kappa>0.60$) between the two radiologists. **Conclusion:** The SS-FSE sequence is performed faster and significantly improves image quality; thus, it should be included into the routine MRCP sequence protocol at 3.0 T. Furthermore, we recommended SS-FSE BH MRCP examination to be applied to uncooperative patients or patients in emergency because of its short acquisition time (1 s).

1. Introduction

Magnetic resonance cholangiopancreatography (MRCP) is a dedicated examination that provides detailed information of the anatomy and pathology of the biliary tree and pancreatic duct (PD) combining cross-sectional and projectional techniques.

Current MRCP techniques use a two-dimensional thick-slab acquisition that usually consists of a single T2-weighted (T2W) image (usually 30–80 mm in slice thickness). This technique obtains rapid breath-hold (BH) (1–4 s) and is free of motions and susceptibility artifacts [1]. Another sequence used is the three-dimensional T2W with thinner sections and without interslice gaps. It has higher signal-to-noise ratio (SNR) and uses postprocessing techniques as multiplanar reconstruction (MPR), maximum intensity projection (MIP), and volume rendering (VR). To date, several groups [2–6] have reported that three-dimensional T2W turbo spin-echo (TSE) MRCP sequences have diagnostic accuracy [2–5,7] similar to that of conventional two-dimensional sequences.

Most of the three-dimensional approaches use respiratory triggering. However, there are disadvantages such as the long acquisition times and constraints on anatomic coverage and spatial resolution. The free-breathing three-dimensional method presents more artifacts

* Corresponding author. Technological Education Institute of Athens, Greece. Tel.: +30 2410 616836; fax: +30 2413501974.
E-mail address: lavdas@med.uth.gr (E. Lavdas).

0899-7071/$ – see front matter © 2013 Elsevier Inc. All rights reserved.
http://dx.doi.org/10.1016/j.clinimag.2013.01.011

than the BH three-dimensional approach, mainly because of blurring from respiratory motion [8].

Parallel imaging techniques were first introduced to reduce scanning time, using the spatial sensitivity information inherent in an array of multiple receiver surface of coils by reducing the number of the time-consuming, phase-encoding steps [9].

High-field whole-body Magnetic Resonance (MR) imaging at 3.0 T has gained substantial interest in recent years. The main benefit of 3.0 T MR scanners, compared with standard 1.5 T MRI scanners is the twofold SNR [10,11]. Therefore, the evaluation of image quality of MRCP at 3.0 T for patients with biliary and pancreatic diseases is considered essential in the clinical practice [12,13].

A few studies have been published comparing MRCP sequences performed at 3.0 T but with a small number of patients in their cohort, mainly healthy volunteers [12,13]. Even less studies compare BH with respiratory-triggered (RT) sequences even at 1.5T [6,14,15]. Therefore, more studies need to be performed in symptomatic patients in order to establish the most appropriate methods of imaging such patients.

We consider that the future of MRCP at 3.0 T with parallel imaging techniques belongs to the BH sequences, since acquisition time is smaller and spatial resolution can be increased.

The purpose of the present study was to evaluate the visibility of the biliary and PD system and the image quality on MRCP images based on two BH methods using array spatial sensitivity encoding technique (ASSET): a single-shot TSE [single-shot fast spin-echo (SS-FSE)] sequence and a three-dimensional single slab fast spin-echo sequence (3D-FSE) [2,16].

2. Materials and methods

2.1. Patients

In the present prospective comparative study, 47 patients (22 males and 25 females; mean age=50 years; age range=22–82 years) that were referred for MRCP during a 12-month period are included. All of them were referred with suspected pancreaticobiliary disease. To null fluid signal in the stomach and duodenum, each patient was given 600 ml of blueberry juice per os (po) 5–10 min before the examination unless there was a contraindication. In 36 patients of these patients, MRCP's results were confirmed by Endoscopic retrograde cholangiopancreatography (ERCP). In the remaining 11 [11] patients, MRCP's results were confirmed by surgery in 5 [5] and by clinical follow-up in 6 [6].

2.2. MR imaging

All MR examinations were performed on a 3.0 T MR scanner (HDxT, GE Medical Systems, USA) using commercially available software on a four-channel body phased-array surface coil as an RF receiver.

Each patient underwent imaging with three coronal oblique MRCP ASSET techniques: respiration-triggered three-dimensional T2 fast spin echo (FSE) sequence with the patient instructed to breathe normally, BH SS-FSE sequence and BH 3D-FSE. In addition, coronal and transverse T2W single-shot FSE sequences were obtained in all patients that covered the upper abdomen from the liver to the kidneys. The calibration scan was acquired separately from the main acquisition.

Two BH sequences with ASSET (factor acceleration 2) were compared. The applied parameters were as follows: repetition time (TR) of auto (mean value=1680 ms), echo time of 570 ms, echo train length of 256, the matrix was 256/384, the 40-mm thick slab, and one excitation. The TR was automatically adjusted by the system with implementation of parallel imaging as a consequence of the reduced echo-train length. Subsequently, a three-dimensional single slab FSE with ASSET factor Acceleration 2 and flow compensation was used. The TR was 1200 ms, the echo time was auto (mean value=550 ms), the echo train length was 22–26, the matrix was160/256, and the thick slab was 22–26 mm. The slice thickness was 3 mm with 50% overlap and one excitation. The acquisition time was 20–25 s for the 3D-FSE sequence and 1 s for each repetition of the SS-FSE sequence. The remaining parameters of the SS-FSE sequence were identical to the 3D-FSE sequence and chemical-selective fat saturation was applied.

2.3. Qualitative evaluation

Two radiologists (E.K. and M.V.) performed monitor readings of the MRCP SS-FSE and 3D-FSE sequences in a double-blinded fashion in a random order. No clinical or demographic information was available to them. Delineation of defined segments of the biliary and pancreatic ductal systems were evaluated by rating the quality of duct visualization using a scoring system [1] on a scale of 1–5 (1=*perfect visualization of the entire ductal structures*; 2=*most of the ductal structures visualized*; 3=*ductal structures partially visible*; 4=*detection of ductal structures almost impossible*; 5=*ductal structures not visible*). The ducts were assessed separately, as follows: (a) extrahepatic bile ducts (EHBDs) including the ampulla and common bile duct (CBD); (b) intrahepatic bile ducts (IHBD); and (c) PD, including head, body, and tail. In addition, the frequency of artifacts was also rated on a scale of 1–5 (1=*no artifacts*; 2=*minimal artifacts*; 3=*minor artifacts*; 4=*major artifacts*; 5=*image not diagnostic due to artifacts*).

Moreover, the pathology of the biliary system was evaluated for 3D-FSE BH sequence from both MIP images and raw data and for SS-FSE BH sequence from MIP images.

2.4. Quantitative evaluation

At the cases that the ducts were visible and could be measured at both sequences, quantitative analysis by measuring the relative signal intensity (rSI) and relative contrast (RC) was performed. Both rSI and RC were identified by placing regions-of-interest (ROIs) between: (a) the intrahepatic bile duct and liver parenchyma; (b) the central portion of the gallbladder and liver parenchyma; (c) the PD and the pancreatic parenchyma; (d) the CBD and the surrounding tissues; (e) the common hepatic duct (CHD) and liver parenchyma; (f) the right hepatic duct (RHD) and liver parenchyma; and (g) the left hepatic duct (LHD) and liver parenchyma.

Relative signal intensity (SI) was calculated according to the following equation: $rSI = SI_{duct}/SI_{adjtiss}$. RC was calculated according to the following equation: $RC = (SI_{duct} - SI_{adjtiss})/(SI_{duct} + SI_{adjtiss})$. SI_{duct} was obtained by placing an ROI within the duct, and the $SI_{adjtiss}$ was obtained by placing an ROI at the normal tissue adjacent to the duct.

The rationale of using rSI instead of the usual SNR was to provide a rough estimate of the overall SI of the image without the possibility of misleading contribution of image noise. Specifically, in parallel imaging techniques, the geometric factor varies over the image and describes local noise enhancements to the final reconstructed image. In this way, the background noise of parallel imaging varies with spatial position [17,18].

The background suppression was evaluated by measuring the signal of the hepatic parenchyma with a representative ROI placed in a region (of healthy parenchyma) without signal from fluid-filled structures or focal lesions.

2.4.1. Statistical analysis

In qualitative evaluation, mean and standard deviation values of image quality scores are provided for each sequence and the Wilcoxon paired signed-ranks test was perform to compare statistically their median differences. In quantitative evaluation, due to the restricted dataset, no normal distribution of the data is assumed and thus all index measurements (rSI, RC) are given as median and interquartile range (IQR) values. The IQR is a robust estimate of the spread of the

Please cite this article as: Lavdas E, et al, How reliable is MRCP with an SS-FSE sequence at 3.0 T: comparison between SS-FSE BH and 3D-FSE BH ASSET sequences, Clin Imaging (2013), http://dx.doi.org/10.1016/j.clinimag.2013.01.011

Table 1
Mean and standard deviation values are provided for each sequence (SS-FSE BH, 3D-FSE BH), radiologist (EK, MV), duct identification (EHBD, IHBD, PD), and artifact identification

	SS-FSE BH	3D-FSE BH	*P*
	Mean±S.D.	Mean±S.D.	
EK			
EHBD	2.04±1.12	2.34±1.31	.123
IHBD[a]	2.63±0.96	3.13±1.33	.016
PD	2.38±1.34	3.40±1.56	<.001
Artifacts	1.72±0.99	2.28±1.38	.006
MV			
EHBD	1.93±1.05	2.32±1.22	.011
IHBD	2.55±0.93	3.13±1.26	.002
PD	2.14±1.33	3.21±1.65	<.001
Artifacts	1.68±0.96	2.28±1.31	.001

The Wilcoxon paired signed-ranks test was performed, and the derived values of *P* indicate statistically significant differences between SS-FSE BH and 3D-FSE BH sequences.
[a] IHBD: intrahepatic bile duct.

data, since changes in the upper and lower 25% of the data do not affect it. If there are outliers in the data, then the IQR is more representative than the standard deviation as an estimate of the spread of the data. To test if the differences between the two sequences are statistically significant, Wilcoxon signed-rank test for paired data was performed. Derived values of $P<.05$ indicate statistically significant differences.

3. Results

3.1. Qualitative analysis

Most of the median differences in the image quality scores obtained with SS-FSE BH sequence compared with those obtained with 3D-FSE BH sequence were highly statistically significant (Table 1). Specifically, image quality of SS-FSE BH sequence for the assessment of EHBD was higher only according to one radiologist (MV, $P<.02$). This finding was statistically significant.

Image quality of SS-FSE BH images was higher for the assessment of IHBD ($P<.02$) and superior for the assessment of PD ($P<.001$), as compared with the images obtained with 3D-FSE BH sequence. Respiratory motion artifacts affected less the quality of images obtained with the SS-FSE BH sequence, than those obtained with the 3D-FSE BH sequence ($P<.01$) (Figs. 1 and 2).

The pathology of the biliary system was evaluated for each of the two MIP images (Table 2). Gallbladder lithiasis was identified in 14/47 patients (29.80%) at SS-FSE MIP images at whom 53 gallbladder stones were counted, while on 3D-FSE MIP images, gallbladder lithiasis was identified in 6/47 patients (12.7%) counting 24 stones (Fig. 3), and on raw data of the 3D-FSE images, gallbladder lithiasis was identified in 8/47 patients (17%) counting 29 stones.

As a whole, CBD pathology was recognized in 16/47 patients (34%). Specifically, at SS-FSE BH MIP images CBD lithiasis was identified in 15/47 patients (31.9%), counting 34 stones, while at 3D-FSE MIP images, lithiasis was identified in 7/47 patients (14.9%), counting 18

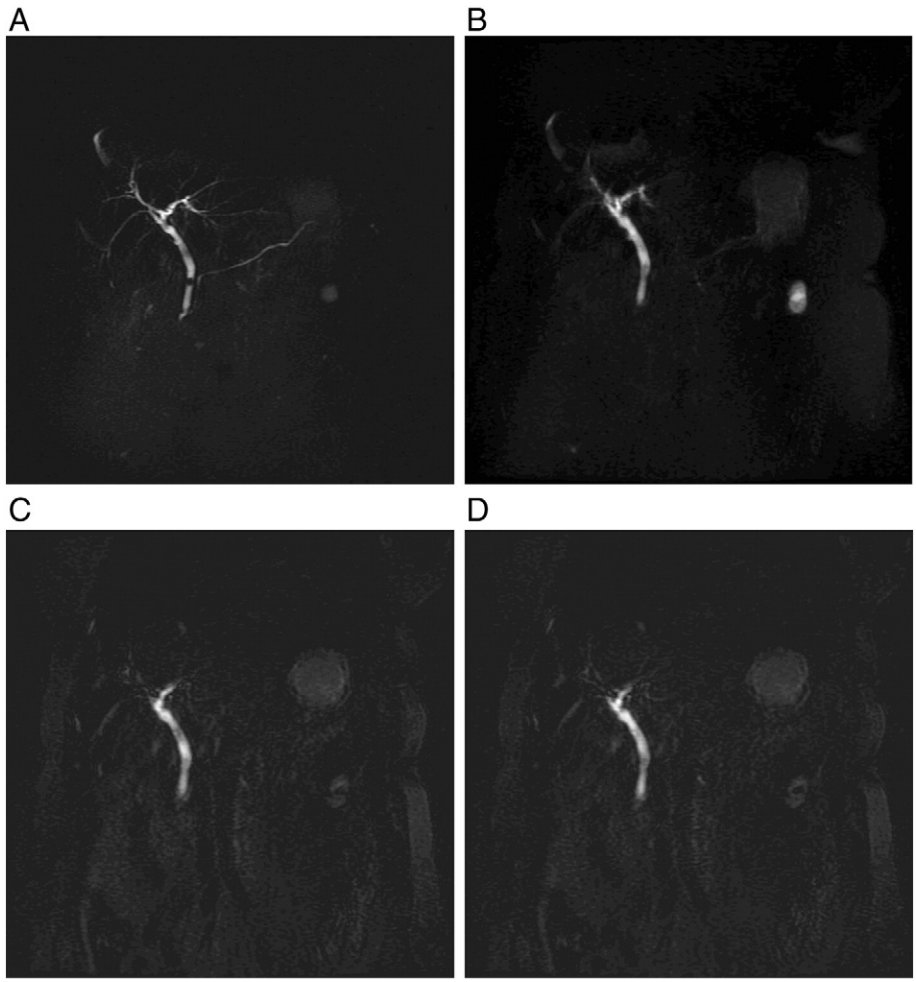

Fig. 1. Comparison of SS-FSE MIP image (A), 3D-FSE MIP images (B), and raw data of the 3D-FSE BH images (C,D) in patient with lithiasis of the CBD. Lithiasis of the CBD is depicted only in SS-FSE BH MIP image, which also shows less motion artifacts and better visualization of the PD and intrahepatic bile duct compared to 3D-FSE images.

Please cite this article as: Lavdas E, et al, How reliable is MRCP with an SS-FSE sequence at 3.0 T: comparison between SS-FSE BH and 3D-FSE BH ASSET sequences, Clin Imaging (2013), http://dx.doi.org/10.1016/j.clinimag.2013.01.011

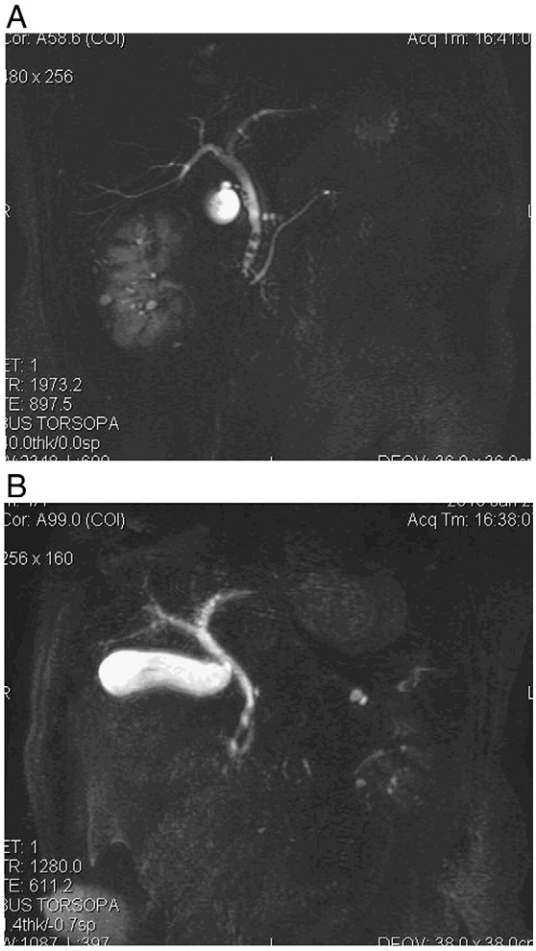

Fig. 2. Images obtained from SS-FSE BH sequence (A) and 3D-FSE BH sequence (B) depict lithiasis of the CBD. The visualization of lithiasis and the PD is better at images obtained from SS-FSE BH sequence, while achieving less motion artifacts.

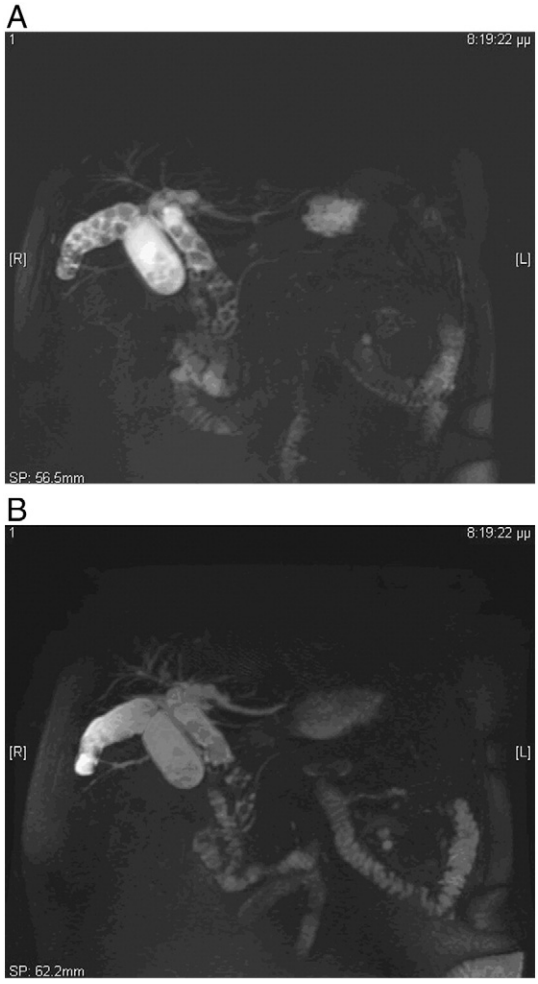

Fig 3. Images obtained from SS-FSE BH sequence (A) and 3D-FSE BH sequence (B) depicting lithiasis within the IHBD, CBD, and gallbladder. SS-FSE BH sequence depicts more stones within the IHBD, CBD, and gallbladder and shows them more clearly compared to 3D-FSE BH sequence.

stones, and on raw data of the 3D-FSE images, lithiasis was identified in 11/47 patients (23%), counting 26 stones. In addition, at SS-FSE MIP images, there was identified a polyp on the CBD wall in 1/47 patient, while at 3D-FSE BH sequence, no polyp was detected from MIP images and raw data (Figs. 1–4).

The results were confirmed by ERCP, surgery, and clinical follow-up. Chololithiasis and choledocholithiasis in each sequence were verified by a percentage ranging between 76% and 93%. The presence of polyp on the CBD was also confirmed. The accuracies between the two sequences for the most common pathologies are presented in Table 3.

With the SS-FSE MIP images, CHD obstruction was identified in 4/47 patients (8.5%), while at 3D-FSE BH sequence, pathology was identified in only 3/47 patients (6.4%) from MIP images and raw data. All four cases with obstruction in CHD were confirmed.

PD straining due to pancreatic head cancer was identified in 4/47 and 1/47 with SS-FSE BH and 3D-FSE BH sequences (from MIP images and raw data), respectively, while PD straining due to chololithiasis was identified in 1/47 patients with the SS-FSE BH sequence only (Fig. 5). All cases with straining of the PD were confirmed.

SS-FSE sequence identified more pathologies in every case compared to 3D-FSE BH sequence.

Table 2
Number of pathologies identified in MRCP using SS-FSE BH and 3D-FSE BH sequences

Lesion	SS-FSE BH number of pts[a] (number of stones)	3D-FSE BH number of pts (number of stones)
Gallbladder lithiasis	14 (53)	6 (24)
CBD lithiasis	15 (34)	7 (18)
CHD obstruction	4	3
PD straining due to pancreatic head cancer	4	1
PD straining due to lithiasis	1 (1)	0
CBD polyp	1	0

[a] pts: patients.

3.2. Quantitative analysis

Table 4 illustrates the results in regard to quantitative analysis. Relative SI and RC was measured both for SS-FSE BH and 3D-FSE BH sequences for a number of anatomical structures from a total of 47 patients, as described in Materials and Methods. For example, IHBD was measured at 30 out of 47 patients, both for SS-FSE BH and 3D-FSE BH sequences. For all anatomical structures that were examined, the median value of rSI and RC in patients in whom SS-FSE BH sequence was performed was higher as compared to the median values of the same anatomical structures in patients performing 3D-FSE BH sequence. This finding was statistically significant ($P<.01$, Wilcoxon signed-rank test with matched pairs).

Saturation for background liver tissue for SS-FSE BH images (6.2 ± 12.8) was statistically significantly superior ($P<.001$, Wilcoxon

Please cite this article as: Lavdas E, et al, How reliable is MRCP with an SS-FSE sequence at 3.0 T: comparison between SS-FSE BH and 3D-FSE BH ASSET sequences, Clin Imaging (2013), http://dx.doi.org/10.1016/j.clinimag.2013.01.011

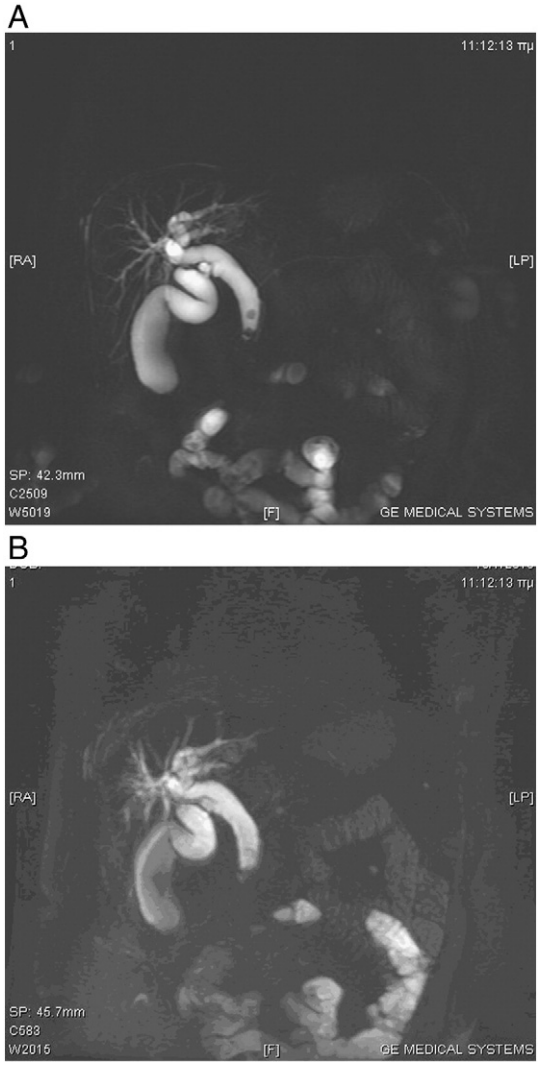

Fig 4. Images obtained from SS-FSE BH sequence (A) and 3D-FSE BH sequence (B) depicting lithiasis of the CBD. Images obtained from SS-FSE BH sequence visualize more clearly the lithiasis and the PD while achieving less motion artifacts. Note better visualization of the stone at the lower part of the CBD at SS-FSE BH, which could be misdiagnosed at 3D-FSE BH.

signed-rank test with matched pairs) than that for 3D-FSE BH images (30.9±9.2).

4. Discussion

MRCP has been routinely performed for more than 15 years facilitating noninvasive imaging of the pancreaticobiliary tree, using heavily T2W sequences. Different magnet strengths (0.5–1.5 Tesla), receiver coils, dimensions (two-dimensional, three-dimensional), breath-holding techniques, and pulse sequences are used in MRCP. The heavily weighted spin-echo sequence, with or without fat suppression, is most frequently employed. Fat suppression is useful in magnetic resonance imaging of the pancreas since fat is the only normal abdominal soft tissue that has a higher signal intensity than the pancreas. In this way, the biliary and PDs appear bright without the need for a contrast material [19].

Parallel imaging techniques are recently used because they achieve a decreased acquisition time without relevant influence on image quality of MRCP [20]. In the past, body imaging has been challenging on high-field whole-body MR imaging at 3.0 T. During the last years, with the development of dedicated receive-only torso array coils, almost all standard whole-body MR examinations have become possible at 3.0 T, leading to a growing interest for routine clinical imaging of the chest, abdomen, and pelvis [18,21–25].

In our routine clinical protocol, we apply 3D-FSE with respiratory triggering, which covers the whole liver and pancreas with an acquisition time of approximately 2.5 min. The BH sequences SS-FSE and 3D-FSE are applied at the main ducts or peripheral ducts according to the findings of the 3D-FSE with respiratory triggering and the SS-FSE axial or coronal sequences.

MRCP at 3.0 T with parallel imaging techniques is better when combined with BH sequences. The RT three-dimensional method produces more artifacts than the BH three-dimensional approach, due to motion artifacts from free respiration. Regardless of the reduction of the acquisition time on RT sequences, the image quality is not improved. On the contrary, the slightest improvement of acquisition time at BH sequences is an important factor for image quality in most patients. In addition, the spatial resolution is increased with 3D-FSE BH sequence especially in patients with the capability for satisfactory BHs, while the same factor with SS-FSE BH sequence is increased in all patients due to the decreased acquisition time. Zhang et al. suggest that BH techniques may be proved to be the method of choice at 3.0 T [8].

The proposed scan parameters by GE for clinical routine for the two BH sequences were used without any change. Both sequences have increased spatial resolution; the 3D-FSE parameters are as follows: slice thickness was 3mm, matrix=160/256, 22–26-mm thick slab, and for the SS-FSE are slice slab 40 mm, matrix=256/384. The thick slab in 3D-FSE was adjusted to the BH capability of the patient (22–26 mm) according to the acquisition time (20–25 s) for the 3D-FSE sequence. Acquisition time for the SS-FSE sequence was 1 s for each repetition.

Relative SI and RC were higher in case of SS-FSE sequence compared to 3D-FSE sequence, as measured at different anatomical structures, and that was statistically significant. One reason for our results is that parallel imaging, when applied to the SS-FSE sequence, achieves increased image saturation for background tissues compared to conventional sequence using a long echo-train length, T2 relaxation sequences due to the reduction of the number of phase-encoding steps and, therefore, the length of the echo train and the duration of the readout period [26–28]. Therefore, the application of parallel imaging will cause a reduction of the T1 component of the signal from the background tissue translating to an increase in RC. The T2 contribution of the background tissue signal is negligible and remains unchanged with parallel imaging [26–28].

Hosseinzadeh et al. [1] studied parallel imaging at two-dimensional-thick-slab MR on 1.5 T and found that there was an improvement on SS-FSE with parallel imaging (ASSET) of the RC ($P<.01$) of fluid-filled to background tissues compared to parallel imaging (SS-FSE) without sensitivity encoding.

In our study, we found that RC was superior ($P<.01$) on SS-FSE with parallel imaging (ASSET) compared to 3D-FSE with parallel imaging (ASSET) at 3.0 T. However, longitudinal relaxation time (T1) and transverse relaxation time (T2) tissues differ between 3.0 T and 1.5 T. Stanisz et al. measured T1 and T2 relaxation in vitro on a variety of animal tissues and found that longitudinal T1 relaxation times increase with the strength of the magnetic field, while T2 relaxation are comparatively field independent from 1.5 to 3.0 T for liver and other tissues [29]. The increase of the longitudinal T1 relaxation times

Table 3
Comparison of accuracies between SS-FSE between SS-FSE BH and 3D-FSE BH sequences

MRCP finding	SS-FSE BH accuracy (%)	3D-FSE BH accuracy (%)
CBD lithiasis	93.6	76.6
CHD obstruction	100	97.9
Pancreatic cancer	97.9	91.5

Please cite this article as: Lavdas E, et al, How reliable is MRCP with an SS-FSE sequence at 3.0 T: comparison between SS-FSE BH and 3D-FSE BH ASSET sequences, Clin Imaging (2013), http://dx.doi.org/10.1016/j.clinimag.2013.01.011

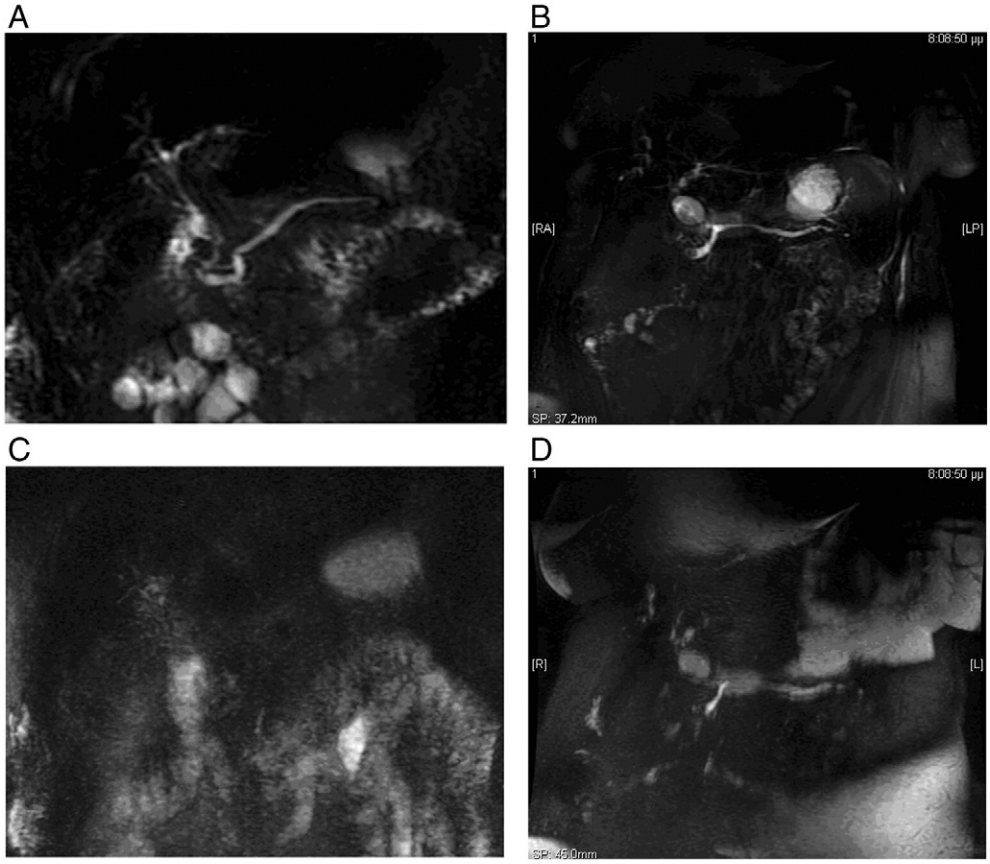

Fig. 5. Images obtained from SS-FSE BH sequence (A,B) and 3D-FSE BH sequence (C,D) acquired from two patients. At the first patient (A,C), image obtained from SS-FSE BH (A) sequence depicts the straining of the PD while at the image obtained from 3D-FSE BH (C) sequence, the straining cannot be identified. Furthermore, the identification of the anatomy of CBD, hepatic duct (HD), and IHD is easier in case of the SS-FSE BH sequence. At the second patient (B,D), images obtained from SS-FSE BH (B) sequence depicts the straining of the PD, caused by lithiasis in the PD, while at images obtained from 3D-FSE BH (D) sequence, the straining is not identified.

at 3.0 T could have contributed to the decrease in signal intensity of the soft tissues other than the biliary tracts and resulted in the improvement of the contrast at 3.0 T.

We consider that another possible explanation for the superior RC on SS-FSE was that the chemical fat suppression performed at 3.0 T can be optimized in order to suppress the signal of fat because the precessional frequency differs between fat protons and water protons and is double at 3.0 T compared to 1.5 T [11]. Specifically for the CBD, better visualization is permitted by the presence of surrounding fat. Moreover, better scaling is achieved in depiction of the tissues because the window's width is linear. Fatty liver and pancreas may also contribute to better visualization of the ductal structures.

However, field inhomogeneities, susceptibility artifacts, and specific absorption rate (SAR) levels limitations are some serious disadvantages of 3T MR imaging. A common approach to overcome the SAR limitations in conventional SE and turbo spin-echo sequences is to prolong the TR [11,30]. This is an even greater problem in 3D-FSE sequences with parallel imaging because a long TR cannot be used [1]. In addition, a long TR on 3D-FSE sequences increases acquisition time, which constitutes an additional disadvantage for BH sequences.

On the contrary, long TR combined with SS-FSE allows a longer recovery interval between readouts in addition to the fixed pause, producing better fluid enhancement because more longitudinal recovery is available for the next readout train [1]. Parallel transmission methods like parallel imaging techniques were shown to be promising for improving B_1 inhomogeneity and reducing the SAR and magnetic susceptibility artifacts [31–33].

Unfortunately, some patients are not able to hold their breath sufficiently. Patients referred for MRCP are frequently in an impaired general condition, often because of pain or an underlying malignant disease and BH examination have to decrease scan acquisition. In many cases, MRCP examination is performed to uncooperative patients or patients who need emergency management. Two-dimensional and free-breathing three-dimensional techniques are probably more robust than the BH three-dimensional technique for patients with limited BH capability [8]. Due to its short acquisition

Table 4
Median and IQR values of index measurements (relative SI, RC)

Anatomic structures	SS-FSE BH		3D-FSE BH		*P*
	Median	IQR	Median	IQR	
Relative SI					
IHBD[a] (n[b]=30)	14.9	11.9	5.0	6.0	<.001
Gallbladder (n=24)	55.5	81.9	13.4	7.7	<.001
PD (n=21)	6.4	5.9	4.7	2.6	.009
CBD (n=36)	6.6	6.8	4.1	3.6	<.001
CHD (n=35)	7.6	9.7	5.0	2.5	<.001
RHD (n=32)	5.8	8.8	3.4	3.0	.002
LHD (n=31)	5.9	7.5	3.5	3.7	<.001
RC					
IHBD (n=30)	0.87	0.11	0.66	0.29	<.001
Gallbladder (n=24)	0.96	0.07	0.86	0.09	<.001
PD (n=21)	0.73	0.25	0.65	0.23	.004
CBD (n=36)	0.74	0.20	0.60	0.25	<.001
CHD (n=35)	0.77	0.18	0.66	0.17	<.001
RHD (n=32)	0.71	0.29	0.54	0.28	.004
LHD (n=31)	0.71	0.27	0.56	0.34	<.001

The Wilcoxon paired signed-ranks test was performed, and the derived values of *P* indicate statistical significance between SS-FSE BH and 3D-FSE BH sequences.

[a] IHBD: intrahepatic bile duct.

[b] n: number of anatomic structures under study.

time, SS-FSE BH (acquisition time: 1 s) may also be applied to all patients and more than one times at the same patient, using different angulation. The increased RC and the diminished respiratory artifacts on SS-FSE is the explanation for better depiction of pathology with this technique.

In addition, in our study, rSI and RC were calculated in more duct segments, compared with other studies. In that way, the results was statistically stronger, and even more, segments of different thickness were included. The superiority of SS-FSE BH comparing with the 3D-FSE BH at all ductal segments is very important because it has thicker thick slab than 3D-FSE BH and partial volume effect is dominant at SS-FSE BH. We believe that using the SS-FSE BH with thinner thick slab (approximately 25 mm) the results may be even better because of the smaller ducts' thickness compared with that of the thick slab.

However, a number of limitations existed in our study. First, the number of distinct pathologies in our series is limited. Second, 3D-FSE had less slab and more thickness, which did not permit full coverage of IHBD and PD (tail segment) while BH duration (acquisition time) was relatively long. This is a controversial issue. Moreover, even minor increases of slab thickness were followed by a further increase of the acquisition time. In addition, in our study, we do not compare the respiration-triggered 3D T2 FSE sequence due to the thick slab; therefore, qualitative measurements would not be objective.

SS-FSE sequence lacks raw data, which does not permit post-processing manipulation of the images with techniques such as MPR, MIP, and VR.

In conclusion, the MRCP at 3.0 T is considered essential and counts a great deal in clinical practice, and therefore, it should be preferred when possible [12,13]. Combination of factors such as high field strengths (3.0 T) magnets, SS-FSE sequence, and parallel imaging techniques greatly increases RC and rSI, which translates into better diagnostic accuracy.

Our findings agree with those performed at lower magnetic fields and suggest that the SS-FSE could be included in the routine MRCP protocols at 3.0 T. However, more studies need to be performed to evaluate the advantages of 3.0 T imaging with clinical trials after altering various parameters (parallel factor acceleration, thick slab, echo-train length and matrix) for depicting even better image quality.

References

[1] Hosseinzadeh K, Furlan A, Almusa O. 2D thick-slab MR holangiopancreatography: does parallel imaging with sensitivity encoding improve image quality and duct visualization? AJR 2008;190(6):W327–34.

[2] Barish MA, Yucel EK, Soto JA, Chuttani R, Ferrucci JT. MR cholangiopancreatography: efficacy of three-dimensional turbo spin-echo technique. AJR 1995;165:295–300.

[3] Soto JA, Barish MA, Yucel EK, Siegenberg D, Ferrucci JT, Chuttani R. Magnetic resonance cholangiography: comparison with endoscopic retrograde cholangiopancreatography. Gastroenterology 1996;110:589–97.

[4] Chan YL, Chan AC, Lam WW, Lee DW, Chung SS, Sung JJ, et al. Choledocholithiasis: comparison of MR cholangiography and endoscopic retrograde cholangiography. Radiology 1996;200:85–9.

[5] Soto JA, Barish MA, Alvarez O, Medina S. Detection of choledocholithiasis with MR cholangiography: comparison of three-dimensional fast spin-echo and single- and multisection half- Fourier rapid acquisition with relaxation enhancement sequences. Radiology 2000;215:737–45.

[6] Soto JA, Barish MA, Yucel EK, Clarke P, Siegenberg D, Chuttani R, et al. Pancreatic duct: MR cholangiopancreatography with a three-dimensional fast spin-echo technique. Radiology 1995;196:459–64.

[7] Pruessmann KP, Weiger M, Scheidegger MB, Boesiger P. SENSE: sensitivity encoding for fast MRI. Magn Reson Med 1999;42(5):952–62.

[8] Zhang J, Israel GM, Hecht EM, Krinsky GA, Babb JS, Lee V. Isotropic 3D T2-weighted MR cholangiopancreatography with parallel imaging: feasibility study. AJR 2006;187:1564–70.

[9] Glockner JF, Hu HH, Stanley DW, Angelos L, King K. Parallel MR imaging: a user's guide. Radiographics 2005;25(5):1279–97.

[10] Schindera MD, Merkle E, Dale BM, Delong DM, Nelson RC. Abdominal magnetic resonance imaging at 3.0 T: what is the ultimate gain in signal-to-noise ratio? Acad Radiol 2006;10:1236–43.

[11] Ramnath RR. 3T MR imaging of the musculoskeletal system (part I): considerations, coils, and challenges. Magn Reson Imaging Clin N Am 2006;14:27–40.

[12] Onishi H, Kim T, Hori M, Murakami T, Tatsumi M, Nakaya Y, Nakamoto A, Osuga K, Tomoda K, Nakamura H. MR cholangiopancreatography at 3.0 T: intraindividual comparative study with MR cholangiopancreatography at 1.5 T for clinical patients. Invest Radiol 2009;44(9):559–65.

[13] Isoda H, Kataoka M, Maetani Y, Kido A, Umeoka S, Tamai K, Koyama T, Nakamoto Y, Miki Y, Saga T, Togashi K. MRCP imaging at 3.0 T vs. 1.5 T: preliminary experience in healthy volunteers. MRI 2007;25(5):1000–6.

[14] Takehara Y. Can MRCP replace ERCP? JMRI 1998;8:517–34.

[15] Barish MA, Soto JA. MR cholangiopancreatography: techniques and clinical applications. AJR 1997;169:1295–303.

[16] Takehara Y, Ichijo K, Tooyama N, Kodaira N, Yamamoto H, Tatami M, Saito M, et al. Breath-hold MR cholangiopancreatography with a long echo train fast spin echo sequence and a surface coil in chronic pancreatitis. Radiology 1994;192:73–8.

[17] Kuhl CK, Gieseke J, von Falkenhausen M, Textor J, Gernert S, Sonntag C, Schild HH. Sensitivity encoding for diffusion-weighted MR imaging at 3.0 T: intraindividual. Radiology 2005;234:517–26.

[18] O'Regan DP, Fitzgerald J, Allsop J, Gibson D, Larkman DJ, Cokkinos D, et al. A comparison of MR cholangiopancreatography at 1.5 and 3.0 Tesla. BJR 2005; 78:894–8.

[19] Silva MA, Munasinghe SH, Munasinghe D, Deen KI. Magnetic resonance cholangiopancreatography (MRCP). Surgery (Oxford) 2002;20(5)120b-120e.

[20] Asbach P, Dewey M, Klessen C, Stemmer A, Ockenga J, Huppertz A, Sander B, Hamm B, Taupitz M. Respiratory-triggered MRCP applying parallel acquisition techniques. JMRI 2006;24(5):1095–100.

[21] Martin DR, Friel HT, Danrad R, De Becker J, Hussain SM. Approach to abdominal imaging at 1.5 Tesla and optimization at 3 Tesla. Magn Reson Imaging Clin N Am 2005;13:241–54.

[22] Sosna J, Rofsky NM, Gaston SM, DeWolf WC, Lenkinski RE. Determinations of prostate volume at 3-Tesla using an external phased array coil: comparison to pathologic specimens. Acad Radiol 2003;10:846–53.

[23] Katz-Brull R, Rofsky NM, Lenkinski RE. Breathhold abdominal and thoracic proton MR spectroscopy at 3T. Magn Reson Med 2003;50:461–7.

[24] Morakkabati-Spitz N, Gieseke J, Kuhl C, Lutterbey G, von Falkenhausen M, Traeber F, et al. 3.0 T high-field magnetic resonance imaging of the female pelvis: preliminary experiences. Eur Radiol 2005;15:639–44.

[25] De Bazelaire CM, Duhamel GD, Rofsky NM, Alsop DC. MR imaging relaxation times of abdominal and pelvic tissues measured in vivo at 3.0 T: preliminary results. Radiology 2004;230:652–9.

[26] Griswold MA, Jacob PM, Chen Q, Goldfarb JW, Manning WJ, Edelman RR, Sodickson DK. Resolution enhancement in single-shot imaging using simultaneous acquisition of spatial harmonics (SMASH). Magn Reson Med 1999;41:1236–45.

[27] Kurihara Y, Yakushiji YK, Tani I, Nakajima Y, Van Cauteren M. Coil sensitivity encoding in MR imaging: advantages and disadvantages in clinical practice. AJR 2002;178:1087–91.

[28] Margolis DJ, Bammer R, Chow LC. Parallel imaging of the abdomen. Top Magn Reson Imaging 2004;15:197–206.

[29] Stanisz GJ, Odrobina EE, Pun J, Escaravage M, Graham SJ, Bronskill MJ, Henkelman RM. T1, T2 relaxation and magnetization transfer in tissue at 3T. Magn Reson Med 2005;54:507–12.

[30] Tetzlaff RH, Mader I, Küker W, Weber J, Ziyeh S, Schulze-Bonhage A, Hennig J, Weigel M. Hyperecho-turbo spin-echo sequences at 3T: clinical application in neuroradiology. Am J Neuroradiol 2008;29:956–61.

[31] Deng W, Yang C, Alagappan V, Wald LL, Boada FE, Stenger VA. Simultaneous z-shim method for reducing susceptibility artifacts with multiple transmitters. Magn Reson Med 2009;61(2):255–9.

[32] Katscher U, Börnert P. Parallel RF transmission in MRI. NMR Biomed 2006;19:393–400.

[33] Lupo JM, Lee MC, Han ET, Cha S, Chang SM, Berger MS, Nelson SJ. Feasibility of dynamic susceptibility contrast perfusion MR imaging at 3T using a standard quadrature head coil and eight-channel phased-array coil with and without SENSE reconstruction. Magn Reson Imaging 2006;24(3):520–9.

Please cite this article as: Lavdas E, et al, How reliable is MRCP with an SS-FSE sequence at 3.0 T: comparison between SS-FSE BH and 3D-FSE BH ASSET sequences, Clin Imaging (2013), http://dx.doi.org/10.1016/j.clinimag.2013.01.011